LETTER

doi:10.1038/nature11929

Differential stem- and progenitor-cell trafficking by prostaglandin E_2

Jonathan Hoggatt[1,2], Khalid S. Mohammad[3]*, Pratibha Singh[1]*, Amber F. Hoggatt[1,4], Brahmananda R. Chitteti[5], Jennifer M. Speth[1], Peirong Hu[1], Bradley A. Poteat[5], Kayla N. Stilger[1], Francesca Ferraro[2], Lev Silberstein[2], Frankie K. Wong[2], Sherif S. Farag[5], Magdalena Czader[6], Ginger L. Milne[7], Richard M. Breyer[8], Carlos H. Serezani[1], David T. Scadden[2], Theresa A. Guise[3], Edward F. Srour[1,5] & Louis M. Pelus[1]

To maintain lifelong production of blood cells, haematopoietic stem cells (HSCs) are tightly regulated by inherent programs and extrinsic regulatory signals received from their microenvironmental niche. Long-term repopulating HSCs reside in several, perhaps overlapping, niches that produce regulatory molecules and signals necessary for homeostasis and for increased output after stress or injury[1–5]. Despite considerable advances in the specific cellular or molecular mechanisms governing HSC–niche interactions, little is known about the regulatory function in the intact mammalian haematopoietic niche. Recently, we and others described a positive regulatory role for prostaglandin E_2 (PGE_2) on HSC function *ex vivo*[6,7]. Here we show that inhibition of endogenous PGE_2 by non-steroidal anti-inflammatory drug (NSAID) treatment in mice results in modest HSC egress from the bone marrow. Surprisingly, this was independent of the SDF-1–CXCR4 axis implicated in stem-cell migration. Stem and progenitor cells were found to have differing mechanisms of egress, with HSC transit to the periphery dependent on niche attenuation and reduction in the retentive molecule osteopontin. Haematopoietic grafts mobilized with NSAIDs had superior repopulating ability and long-term engraftment. Treatment of non-human primates and healthy human volunteers confirmed NSAID-mediated egress in other species. PGE_2 receptor knockout mice demonstrated that progenitor expansion and stem/progenitor egress resulted from reduced E-prostanoid 4 (EP4) receptor signalling. These results not only uncover unique regulatory roles for EP4 signalling in HSC retention in the niche, but also define a rapidly translatable strategy to enhance transplantation therapeutically.

Mice were treated with the prototypical NSAID indomethacin (Supplementary Fig. 1a) to reduce endogenous PGE_2 production, resulting in a significant increase in haematopoietic progenitor cells (HPCs) in the peripheral blood that was not accompanied by an increase in the number of white blood cells (Supplementary Fig. 1b, c). This HPC increase but unaltered white blood cell count probably accounts for the lack of previous detection of this observation, despite decades of clinical NSAID use. No increase in HPC egress was seen in mice treated with the lipoxygenase inhibitor baicalein, suggesting a cyclooxygenase (COX) pathway-specific effect. Co-administration of indomethacin with the clinically used mobilizing agent granulocyte colony-stimulating factor (G-CSF) significantly enhanced (~twofold) HPC mobilization (Supplementary Fig. 1b). NSAIDs with varying degrees of COX-1 and COX-2 selectivity demonstrated significant mobilization with indomethacin, aspirin, ibuprofen and meloxicam (Supplementary Fig. 2). Meloxicam inhibits both COX-1 and COX-2 in the bone marrow microenvironment (Supplementary Fig. 3), and when compared to other dual inhibitors it has a reduced incidence of gastrointestinal discomfort[8] and inhibition of platelet aggregation[9]. Therefore, meloxicam was used in most of the studies. We did not extensively test the differential roles of

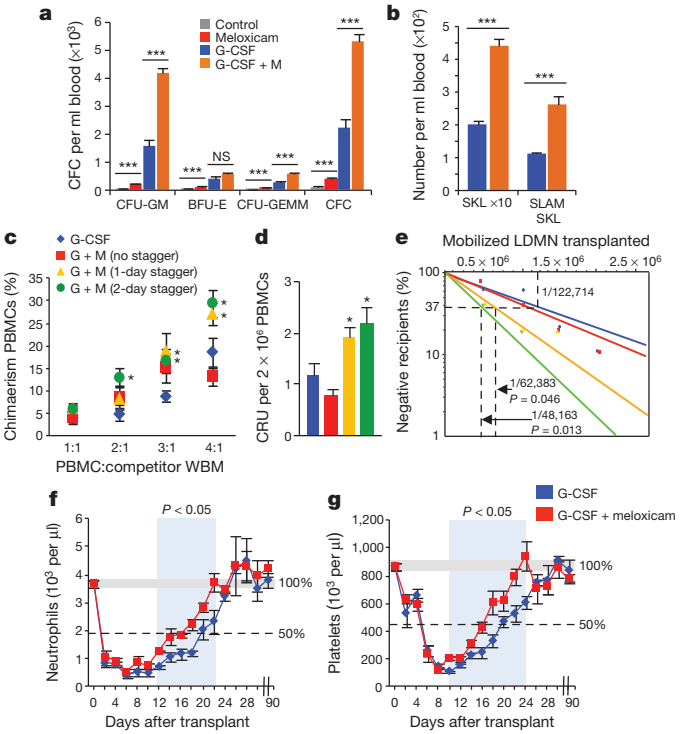

Figure 1 | NSAIDs mobilize haematopoietic stem and progenitor cells. **a**, **b**, Meloxicam enhances mobilization of HPCs (**a**) and HSCs (**b**) into blood ($n = 4$–5 mice per group per experiment; three experiments). BFU-E, erythroid progenitors (burst-forming unit–erythrocyte); CFC, colony-forming cells; CFU-GEMM, multipotential progenitor cells (colony-forming unit–granulocyte, erythrocyte, macrophage, megakaryocyte); M, meloxicam. **c**, Chimaerism. PBMCs, peripheral blood mononuclear cells; WBM, whole bone marrow cells. **d**, **e**, Competitive repopulating units (CRU) (**d**), and LT-HSC frequency (Poisson distribution) (**e**), 36 weeks after limiting dilution competitive transplants of PBMCs from mice treated with G-CSF and combination regimens ($n = 8$ mice per group, assayed individually). Mice were treated with G-CSF or a staggered regimen of G-CSF plus meloxicam, and PBMCs were transplanted into lethally irradiated mice. **f**, **g**, Neutrophil (**f**) and platelet (**g**) recovery were monitored for 90 days. $^*P < 0.05$, $^{**}P < 0.01$, $^{***}P < 0.001$; unpaired two-tailed t-test. All data are mean ± s.e.m.

[1]Microbiology and Immunology, Indiana University School of Medicine, Indianapolis, Indiana 46202, USA. [2]Stem Cell and Regenerative Biology, Harvard University/Harvard Stem Cell Institute/Harvard Medical School/Center for Regenerative Medicine, Massachusetts General Hospital, Boston, Massachusetts 02114, USA. [3]Medicine/Endocrinology, Indiana University School of Medicine, Indianapolis, Indiana 46202, USA. [4]Biologic Resources Laboratory, University of Illinois at Chicago, Chicago, Illinois 60612, USA. [5]Medicine/Division of Hematology and Oncology, Indiana University School of Medicine, Indianapolis, Indiana 46202, USA. [6]Pathology and Laboratory Medicine, Indiana University School of Medicine, Indianapolis, Indiana 46202, USA. [7]Eicosanoid Core Laboratory, Division of Clinical Pharmacology, Vanderbilt University, Nashville, Tennessee 37232, USA. [8]Division of Nephrology and Hypertension, Vanderbilt University, Nashville, Tennessee 37232, USA.
*These authors contributed equally to this work.

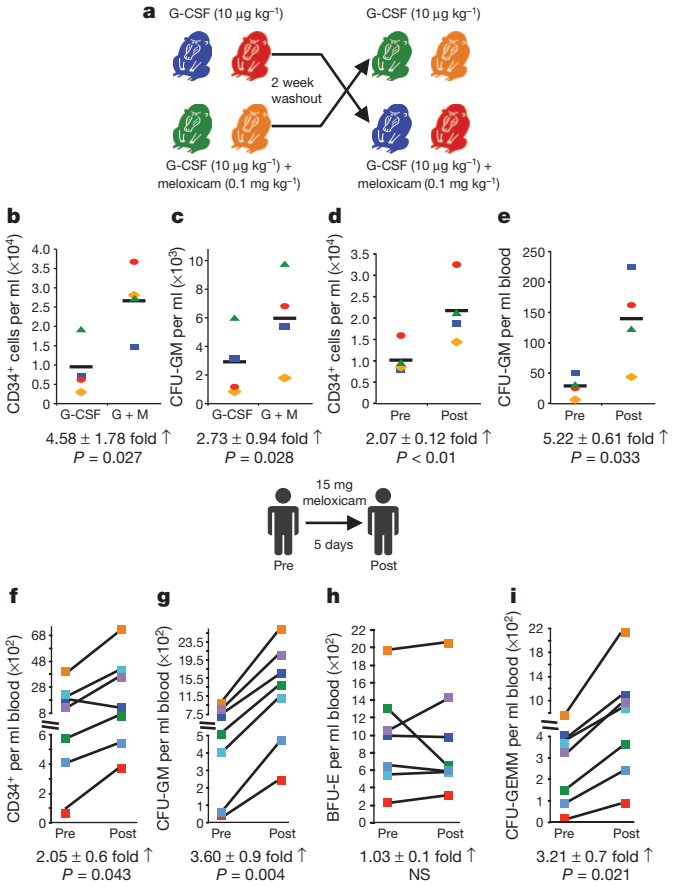

Figure 2 | Non-human primates and healthy human volunteers mobilize HSCs and HPCs in response to NSAID treatment. **a**–**e**, Four baboons were treated with G-CSF with/without meloxicam in a crossover design (shown in **a**). **b**, **c**, $CD34^+$ cells (**b**) and CFU-GM (**c**) in peripheral blood were determined. **d**, **e**, $CD34^+$ cells (**d**) and CFU-GM (**e**) in peripheral blood were determined before (pre) and after (post) five days of meloxicam treatment. **f**–**i**, Seven healthy human volunteers were treated with 15 mg meloxicam a day orally for five days, and assessed for $CD34^+$ cells (**f**), CFU-GM (**g**), BFU-E (**h**) and CFU-GEMM (**i**), before and after treatment. Statistics represent paired, two-tailed *t*-test; NS, not significant.

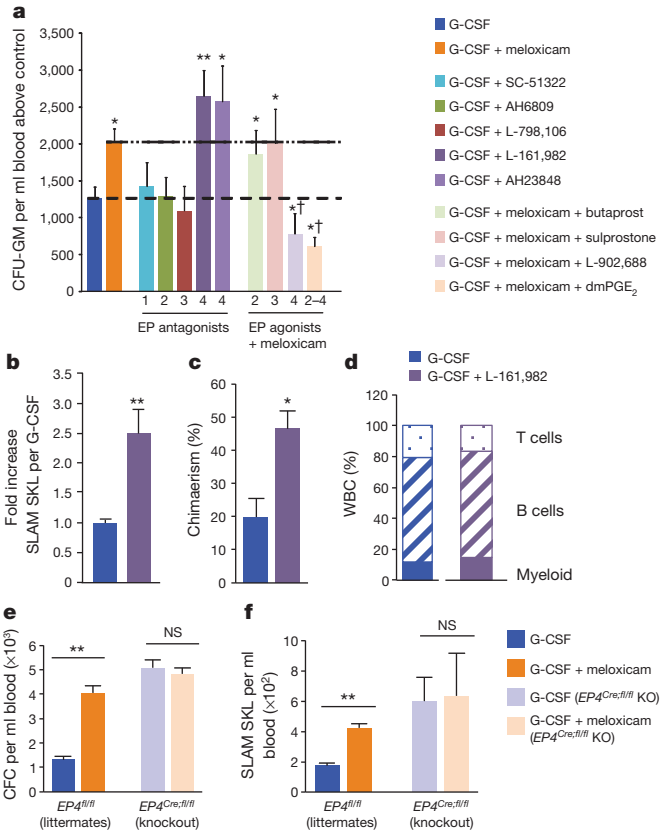

Figure 3 | PGE_2 EP4 receptor antagonism/knockout expands bone marrow HPCs and enhances mobilization. **a**, HPC mobilization with G-CSF, G-CSF plus meloxicam, G-CSF plus E-prostanoid (EP) receptor antagonists, or G-CSF, meloxicam and E-prostanoid receptor agonists ($n = 5$ mice per group, assayed individually). **b**–**d**, The EP4 antagonist L-161,982 enhanced HSC mobilization ($n = 4$ mice per group, assayed individually) (**b**), and long-term reconstitution 16 weeks after transplantation (**c**), with multi-lineage reconstitution ($n = 5$ mice per group, assayed individually) (**d**). WBC, white blood cells. **e**, **f**, EP4 knockout mobilization. Meloxicam enhances mobilization of HPCs (**e**) and SLAM SKL cells (**f**) in wild-type littermates ($EP4^{fl/fl}$), but not in EP4 conditional knockouts ($EP4^{Cre;fl/fl}$ KO) ($n = 3$–4 mice per group, assayed individually). $^*P < 0.05$, $^{**}P < 0.01$, $^{***}P < 0.001$; unpaired two-tailed *t*-test. $^\dagger P < 0.05$ compared to G-CSF plus meloxicam. All data are mean ± s.e.m.

COX-1 and COX-2 and, therefore, there may be similar activity of NSAIDs with different COX-1 or COX-2 inhibitory profiles when compared to meloxicam.

Meloxicam, similar to indomethacin, increased the egress of HPCs (Fig. 1a and Supplementary Fig. 4) and the phenotypic HSC-enriched populations $Sca\text{-}1^+$ $c\text{-}kit^+$ Lin^- (SKL) or the highly purified $CD150^+$ $CD48^-$ (SLAM) SKL populations (Fig. 1b and Supplementary Fig. 4). Enhanced cell egress was maintained in *Alox5* (also known as *5LX* and *5-ALOX*) knockout mice (Supplementary Fig. 5), further demonstrating that the effects are not due to general eicosanoid inhibition. Enhancement in cell egress was also not specific to G-CSF, as meloxicam enhanced the cell mobilization caused by the clinically used CXCR4 antagonist AMD3100 (Supplementary Fig. 6).

Despite significant increases in phenotypic HSCs and functional HPCs in the peripheral blood, two early transplant attempts did not show enhanced HSC engraftment (Supplementary Fig. 7a, b). Because we previously showed that PGE_2 signalling was a positive regulator of HSC CXCR4 expression and homing to the niche[6], we proposed that although the HSC and HPC yield was increased in NSAID grafts, CXCR4 expression might be reduced, accounting for the apparent lack of enhanced engraftment. To test this hypothesis we staggered the administration of NSAID and G-CSF to allow for haematopoietic mobilization and restoration of normal endogenous PGE_2 signalling before transplantation (Supplementary Fig. 7c). CXCR4 levels were significantly lower after NSAID treatment, and staggered administration allowed for restored receptor levels, while maintaining enhanced HSC egress (Supplementary Fig. 7d, e). We competitively transplanted mobilized grafts from G-CSF, or non-staggered and staggered G-CSF plus meloxicam-treated mice. Staggered administration resulted in significant enhancement of long-term repopulating HSC (LT-HSC) engraftment, with a 48-h stagger resulting in a 2.6-fold increase in LT-HSCs (Fig. 1c–e and Supplementary Fig. 8). When grafts were transplanted non-competitively, staggered co-administration of meloxicam resulted in four-day faster recovery of neutrophils (Fig. 1f) and platelets (Fig. 1g) compared with G-CSF alone. Secondary transplantation confirmed sustained LT-HSC activity with multi-lineage reconstitution 36 weeks after transplant (Supplementary Fig. 9).

To confirm NSAID-mediated HSC and HPC egress in other species, four baboons were treated with a standard regimen of G-CSF, or with the combination of G-CSF plus meloxicam in a crossover design (Fig. 2a). Although the responses of individual baboons to G-CSF varied, in all cases meloxicam treatment increased $CD34^+$ cells (Fig. 2b) and granulocytic–monocytic progenitors (colony-forming unit-granulocyte, macrophage; CFU-GM) (Fig. 2c) in peripheral blood. Meloxicam treatment on its own also resulted in significant

HSC and HPC egress (Fig. 2d, e). In healthy human volunteers, meloxicam treatment resulted in significant increases in $CD34^+$ cells (Fig. 2f), and functionally defined HPCs (Fig. 2g–i), matching the HSC and HPC egress seen with meloxicam treatment in baboons and mice. Thus, short-term endogenous PGE_2 inhibition, closely resembling current clinical NSAID treatment, results in a previously unappreciated increase in HSC and HPC mobilization.

Meloxicam treatment increased functionally defined myeloid progenitors and phenotypically defined granulocyte–macrophage progenitors in the bone marrow, but no differences in phenotypically or functionally defined HSC were observed (Supplementary Fig. 10). Because PGE_2 signals through four receptors (EP1–4), each with unique signalling pathways[10], we proposed that the myeloid expansion and egress was due to lack of signalling via one or more of the E-prostanoid receptors. Only agonists capable of activating the EP4 receptor inhibited myeloid HPCs (Supplementary Fig. 11a). To confirm further the specific role of the EP4 receptor, similar assays were performed using knockout mice for each of the E-prostanoid receptors. Comparison of all knockout strains showed that only HPCs from conditional $EP4^{-/-}$ (also known as $Ptger4^{-/-}$) mice had reduced responses to inhibition by PGE_2 (Supplementary Fig. 11b), and a 2.3-fold increase in marrow macrophage progenitors (colony-forming unit-macrophage; CFU-M) compared to wild type (Supplementary Fig. 11c). Co-administration of EP4 antagonists with G-CSF significantly enhanced mobilization, similar to meloxicam, whereas EP1, EP2 and EP3 antagonists failed to increase mobilization (Fig. 3a). Furthermore, when a selective EP4 agonist was co-administered with G-CSF plus meloxicam, the meloxicam enhancement of mobilization was abrogated, and to the same degree as co-administration of the long-acting PGE_2 analogue 16,16-dimethyl-PGE_2 ($dmPGE_2$). Agonists that did not target the EP4 receptor failed to alter meloxicam enhancement. EP4 antagonism with G-CSF enhanced mobilization of LT-HSCs (Fig. 3b–d), indicating that the NSAID-mediated effects on HPC/HSC egress are due to reduced EP4 receptor signalling. Consistent with pharmacological data, conditional *EP4* deletion increased HPC and HSC egress (Supplementary Fig. 11d–f), and enhanced mobilization caused by meloxicam was abrogated (Fig. 3e, f). These data implicate PGE_2 and EP4 receptor signalling in mediating the cell egress effects of NSAIDs; however, because we did not conduct a comprehensive lipidomic profile we cannot exclude contributions of other eicosanoids.

In vitro and *in vivo* results indicate that a lack of EP4 signalling drives HPC expansion, possibly explaining one mechanism responsible for the enhanced HPC egress: more marrow HPCs allows more to

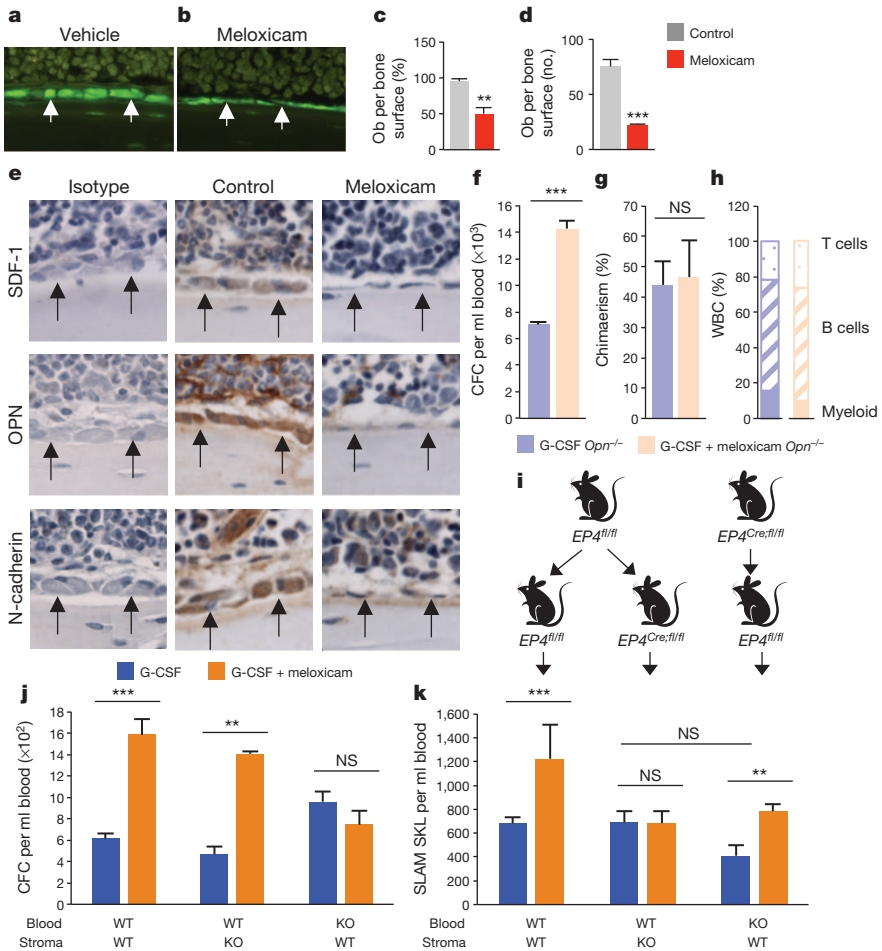

Figure 4 | NSAIDs attenuate haematopoietic supportive molecules and differentially mobilize HSCs and HPCs in *Opn* knockout and *EP4* conditional knockout mice. **a**–**d**, Assessment of Col2.3-GFP cells after vehicle (**a**) or meloxicam (**b**) demonstrates reduced percentages (**c**) and numbers (**d**) of osteolineage cells (expressed as the percentage/number of osteoblasts (ob) per bone surface) ($n = 4$ mice per group, assayed individually). **e**, Immunohistochemical staining of haematopoietic supportive molecules after treatment with meloxicam (original magnification, ×400). Arrows denote osteolineage cell layer lining the endosteum. **f**–**h**, Meloxicam enhances mobilization of HPCs in $Opn^{-/-}$ mice (**f**), with no enhancement in long-term reconstitution 16 weeks after transplantation (**g**, **h**). **i**, Representation of chimaera generation allowing conditional knockout of donor haematopoietic cells, or recipient stromal cells. *EP4* was deleted with tamoxifen 8 weeks after transplantation and mice were treated with G-CSF or G-CSF plus meloxicam. **j**, **k**, Enhanced mobilization of HPCs by meloxicam when EP4 is expressed on haematopoietic cells (**j**) and enhanced mobilization of HSCs when EP4 is expressed by stromal cells (**k**) ($n = 4$ mice per group, assayed individually). WT, wild type. $^*P < 0.05$, $^{**}P < 0.01$, $^{***}P < 0.001$; unpaired two-tailed *t*-test. Data are mean ± s.e.m.

be mobilized to the periphery. However, no alterations in bone marrow HSC content were observed (Supplementary Fig. 10), suggesting that HSC mobilization results from a different mechanism, perhaps acting on the HSC niche. Gross histological analysis of NSAID-treated mice over 0–4 days showed a progressive increase in the laminarity of osteolineage cells lining the endosteum (Supplementary Figs 12 and 13), similar to that seen after G-CSF treatment[11]. Comparable results were observed in collagen 2.3-GFP reporter mice (which express the enhanced green fluorescent protein gene 2.3 kilobases upstream of the rat *Col1a1* promoter), showing marked attenuation of osteolineage cells (Fig. 4a–d), and in mice after conditional *EP4* deletion (Supplementary Fig. 14). Dynamic bone formation assays using staggered calcein double labelling and modified Goldner's trichrome staining support significant attenuation of osteolineage cellular function (Supplementary Fig. 15).

At present there is considerable debate about the direct or indirect roles of osteoclasts in haematopoietic niche regulation and HSC or HPC retention (reviewed in refs 12 and 13). To assess the role of osteoclasts, mice were treated with meloxicam and/or G-CSF with or without zoledronic acid, a potent inhibitor of osteoclast activity[14]. Similar to a recent report[15], zoledronic acid resulted in an increase in HSC or HPC mobilization by meloxicam and G-CSF (Supplementary Fig. 16), suggesting that increased osteoclast activity is not a mitigating mechanism for NSAID-mediated HSC and HPC egress. Niche attenuation and HSC or HPC mobilization by G-CSF have recently been reported to be mediated by marrow-resident monocyte/macrophage populations[15–17]. In contrast to G-CSF[15], immunohistochemical analysis demonstrated that meloxicam does not reduce F4/80^{+} macrophages (Supplementary Fig. 17a), nor is there a reduction in phenotypically defined macrophages assessed by flow cytometry (Supplementary Fig. 17b, c). We observed no changes in sinusoidal endothelial cell number or apoptotic state (Supplementary Fig. 18), nor sinusoid vessels or endothelial cell number by immunohistochemistry (Supplementary Fig. 19). Similarly, there was no alteration in the nestin^{+} cell number (Supplementary Fig. 20). No differences in marrow MMP-9 or soluble c-kit, agents reported to regulate HSC motility in the bone marrow niche[18], were observed in NSAID-treated mice (data not shown), suggesting other unique HSC-retentive molecule(s) are regulated by EP4.

We fractionated osteolineage cells into three sub-populations[19,20] (Supplementary Fig. 21a). Quantitative PCR with reverse transcription (qRT–PCR) analysis revealed that all three populations expressed all four E-prostanoid receptors, with EP4 being expressed most predominately (Supplementary Fig. 21b). Meloxicam treatment resulted in reductions in messenger RNA expression of several haematopoietic supportive molecules, including *Jag1*, *Runx2*, *Vcam1*, *SCF* (also known as *Kitl*), *SDF-1* (*Cxcl12*), and osteopontin (*Opn*, also known as *Spp1*) (Supplementary Fig. 21c). Similarly, immunohistochemistry staining demonstrated reductions in SDF-1, OPN and N-cadherin expression (Fig. 4e). Analysis in *EP4* conditional knockout mice showed a significant reduction in mesenchymal progenitor cells compared to Cre(−) littermates and wild-type controls (Supplementary Fig. 21d), further demonstrating a role for EP4 signalling in haematopoietic niche maintenance.

Because the interaction of SDF-1 with its cognate receptor CXCR4 is a well-known mediator of niche retention, we sought to determine whether reduced expression of SDF-1 mediated the HSC and HPC egress caused by NSAID treatment. Surprisingly, despite the robust egress of cells in *Cxcr4* conditional knockout mice, both HPC and HSC trafficking to the periphery were significantly enhanced by meloxicam (Supplementary Fig. 22). Osteopontin has been reported as a regulator of both HSC quiescence[21] and niche retention[22]. In contrast to CXCR4, when *Opn* knockout mice were treated with meloxicam or G-CSF for six days, meloxicam enhanced the mobilization of HPCs (Fig. 4f), but, unexpectedly, not of HSCs (Fig. 4g, h; additional data in Supplementary Fig. 23), whereas both HPCs and HSCs were mobilized by G-CSF in wild-type mice. This surprising result indicates that NSAID-mediated OPN reduction is specifically responsible for the observed HSC niche egress, whereas the increased number of peripheral HPCs results from an independent mechanism(s). To determine the differential roles of haematopoietic intrinsic versus stromal niche EP4 signalling in mediating HPC/HSC egress, we created chimaeric mice in which we could conditionally delete *EP4* from donor haematopoietic cells or recipient stromal cells (Fig. 4i). EP4 expression on haematopoietic cells was required for NSAID-mediated egress of HPCs (Fig. 4j), whereas EP4 on stromal cells was specifically necessary for HSC egress (Fig. 4k). These studies demonstrate that PGE_2 signalling differentially regulates HPC and HSC retention in the bone marrow through both cell intrinsic and cell extrinsic mechanisms, and future studies should define the relative roles of individual stromal niche cell contributions to EP4-mediated niche retention. To our knowledge, this is the first report of an agent capable of mobilizing both HSCs and HPCs and doing so through cell-stage-specific mechanisms.

METHODS SUMMARY

C57Bl/6 and *Opn*$^{-/-}$ mice were purchased from Jackson Laboratories. B6.SJL-PtrcAPep3B/BoyJ mice were bred in-house. *Cxcr4*$^{flox/flox}$ mice were generated as described[23] and were a gift from Y. R. Zou. *EP1*$^{-/-}$ (also known as *Ptger1*$^{-/-}$), *EP2*$^{-/-}$ (*Ptger2*$^{-/-}$), *EP3*$^{-/-}$ (*Ptger3*$^{-/-}$), and *EP4*$^{flox/flox}$ mice were generated as described[24–26]. Conditional mice were bred to *Ubc-Cre/ERT2* mice from Jackson. Female olive baboons (*Papio Anubis*) were housed individually in conventional caging of the Biological Resources Laboratory, University of Illinois at Chicago. Primate research was approved by the University of Illinois Animal Care and Use Committee (IACUC). The IACUC of the Indiana University School of Medicine (IUSM) approved all protocols. The Institutional Review Board of IUSM approved human subject research and informed consent was acquired from all volunteers.

Full Methods and any associated references are available in the online version of the paper.

Received 6 May 2012; accepted 22 January 2013.
Published online 13 March 2013.

1. Calvi, L. M. *et al.* Osteoblastic cells regulate the haematopoietic stem cell niche. *Nature* **425,** 841–846 (2003).
2. Ding, L., Saunders, T. L., Enikolopov, G. & Morrison, S. J. Endothelial and perivascular cells maintain haematopoietic stem cells. *Nature* **481,** 457–462 (2012).
3. Méndez-Ferrer, S. *et al.* Mesenchymal and haematopoietic stem cells form a unique bone marrow niche. *Nature* **466,** 829–834 (2010).
4. Raaijmakers, M. H. *et al.* Bone progenitor dysfunction induces myelodysplasia and secondary leukaemia. *Nature* **464,** 852–857 (2010).
5. Zhang, J. *et al.* Identification of the haematopoietic stem cell niche and control of the niche size. *Nature* **425,** 836–841 (2003).
6. Hoggatt, J., Singh, P., Sampath, J. & Pelus, L. M. Prostaglandin E_2 enhances hematopoietic stem cell homing, survival, and proliferation. *Blood* **113,** 5444–5455 (2009).
7. North, T. E. *et al.* Prostaglandin E_2 regulates vertebrate haematopoietic stem cell homeostasis. *Nature* **447,** 1007–1011 (2007).
8. Ahmed, M., Khanna, D. & Furst, D. E. Meloxicam in rheumatoid arthritis. *Expert Opin. Drug Metab. Toxicol.* **1,** 739–751 (2005).
9. Rinder, H. M. *et al.* Effects of meloxicam on platelet function in healthy adults: a randomized, double-blind, placebo-controlled trial. *J. Clin. Pharmacol.* **42,** 881–886 (2002).
10. Breyer, R. M., Bagdassarian, C. K., Myers, S. A. & Breyer, M. D. Prostanoid receptors: subtypes and signaling. *Annu. Rev. Pharmacol. Toxicol.* **41,** 661–690 (2001).
11. Katayama, Y. *et al.* Signals from the sympathetic nervous system regulate hematopoietic stem cell egress from bone marrow. *Cell* **124,** 407–421 (2006).
12. Bethel, M., Srour, E. F. & Kacena, M. A. Hematopoietic cell regulation of osteoblast proliferation and differentiation. *Curr. Osteoporos. Rep.* **9,** 96–102 (2011).
13. Hoggatt, J. & Pelus, L. M. Many mechanisms mediating mobilization: an alliterative review. *Curr. Opin. Hematol.* **18,** 231–238 (2011).
14. Mundy, G. R., Yoneda, T. & Hiraga, T. Preclinical studies with zoledronic acid and other bisphosphonates: impact on the bone microenvironment. *Semin. Oncol.* **28,** 35–44 (2001).
15. Winkler, I. G. *et al.* Bone marrow macrophages maintain hematopoietic stem cell (HSC) niches and their depletion mobilizes HSCs. *Blood* **116,** 4815–4828 (2010).
16. Chow, A. *et al.* Bone marrow CD169^{+} macrophages promote the retention of hematopoietic stem and progenitor cells in the mesenchymal stem cell niche. *J. Exp. Med.* **208,** 261–271 (2011).
17. Christopher, M. J., Rao, M., Liu, F., Woloszynek, J. R. & Link, D. C. Expression of the G-CSF receptor in monocytic cells is sufficient to mediate hematopoietic progenitor mobilization by G-CSF in mice. *J. Exp. Med.* **208,** 251–260 (2011).
18. Heissig, B. *et al.* Recruitment of stem and progenitor cells from the bone marrow niche requires MMP-9 mediated release of Kit-ligand. *Cell* **109,** 625–637 (2002).

19. Chitteti, B. R. *et al.* Impact of interactions of cellular components of the bone marrow microenvironment on hematopoietic stem and progenitor cell function. *Blood* **115,** 3239–3248 (2010).
20. Nakamura, Y. *et al.* Isolation and characterization of endosteal niche cell populations that regulate hematopoietic stem cells. *Blood* **116,** 1422–1432 (2010).
21. Stier, S. *et al.* Osteopontin is a hematopoietic stem cell niche component that negatively regulates stem cell pool size. *J. Exp. Med.* **201,** 1781–1791 (2005).
22. Grassinger, J. *et al.* Thrombin-cleaved osteopontin regulates hemopoietic stem and progenitor cell functions through interactions with $\alpha_9\beta_1$ and $\alpha_4\beta_1$ integrins. *Blood* **114,** 49–59 (2009).
23. Nie, Y. *et al.* The role of CXCR4 in maintaining peripheral B cell compartments and humoral immunity. *J. Exp. Med.* **200,** 1145–1156 (2004).
24. Kennedy, C. R. *et al.* Salt-sensitive hypertension and reduced fertility in mice lacking the prostaglandin EP_2 receptor. *Nature Med.* **5,** 217–220 (1999).
25. Guan, Y. *et al.* Antihypertensive effects of selective prostaglandin E_2 receptor subtype 1 targeting. *J. Clin. Invest.* **117,** 2496–2505 (2007).
26. Schneider, A. *et al.* Generation of a conditional allele of the mouse prostaglandin EP4 receptor. *Genesis* **40,** 7–14 (2004).

Supplementary Information is linked to the online version of the paper at www.nature.com/nature.

Acknowledgements These studies were supported by National Institutes of Health (NIH) grants HL096305 (L.M.P.), CA143057, CA069158 (T.A.G., K.S.M.), HL100402 (D.T.S.) and DK37097 (R.M.B.). J.H. was supported by NIH training grants DK07519, HL07910 and HL087735. Flow cytometry was performed in the Flow Cytometry Resource Facility of the Indiana University Simon Cancer Center (NCI P30 CA082709). Additional core support was provided by a Center of Excellence in Hematology grant P01 DK090948. The authors would like to thank H. E. Broxmeyer and B. Saez for critically reading the manuscript.

Author Contributions All authors assisted in writing of the manuscript. J.H. analysed data, wrote the manuscript, designed all experiments and implemented all experiments with assistance from P.S., A.F.H., B.R.C., J.M.S., P.H., B.A.P., K.N.S., F.F., L.S. and F.K.W. K.S.M., M.C. and T.A.G. performed histological analyses and assisted with corresponding study designs. G.L.M. and R.M.B. performed eicosanoid analysis and generated E-prostanoid receptor knockout mice, and C.H.S. assisted with *Alox5* mice and experiments. D.T.S. and E.F.S. assisted with experimental design and data analyses. L.M.P. designed and performed experiments, analysed and evaluated all data, and wrote the manuscript.

Author Information Reprints and permissions information is available at www.nature.com/reprints. The authors declare competing financial interests: details accompany the full-text HTML version of the paper at www.nature.com/nature. Readers are welcome to comment on the online version of the paper. Correspondence and requests for materials should be addressed to L.M.P. (lpelus@iupui.edu).

METHODS

Animals and subjects. C57Bl/6 (CD45.2) mice were purchased from Jackson Laboratories (Bar Harbour). B6.SJL-PtrcAPep3B/BoyJ (BOYJ) (CD45.1) mice were bred in-house. *Cxcr4*$^{flox/flox}$ mice were generated as described[23] and were a gift from Y.-R. Zou. *EP1*$^{-/-}$ (also known as *Ptger1*$^{-/-}$), *EP2*$^{-/-}$ (*Ptger2*$^{-/-}$), *EP3*$^{-/-}$ (*Ptger3*$^{-/-}$), and *EP4*$^{flox/flox}$ mice were generated as described[24–26]. *Opn*$^{-/-}$ mice were purchased from Jackson Laboratories. *Nestin-GFP*[27], *Col2.3-GFP*[28] and *Alox5* (ref. 29) mice were generated as described. *EP4*$^{flox/flox}$ mice were bred to *Ubc-Cre/ERT2* mice from Jackson Laboratories to generate conditional *EP4* knockout mice. All mice were maintained on a C57Bl/6 background. Female olive baboons (*Papio Anubis*), within the weight range of 16–19 kg, were housed individually in conventional caging and holding rooms of the Biological Resources Laboratory, a centralized animal facility for the University of Illinois at Chicago Medical Center. The conducted primate research was approved by the University of Illinois at Chicago Animal Care and Use Committee. The Animal Care and Use Committee of Indiana University School of Medicine (IUSM) approved all protocols, and the Institutional Review Board approved human subject research. Informed consent was obtained from all volunteers.

Peripheral blood and bone marrow acquisition and processing. Peripheral blood from mice was obtained by cardiac puncture after CO_2 asphyxiation using an EDTA-rinsed syringe. Blood was transferred to tubes containing EDTA for complete blood cell (CBC) analysis. CBC analysis was performed on a Hemavet 950FS (Drew Scientific). PBMCs were prepared by centrifugation over lympholyte mammal (Cedarlane Laboratories) at 800 *g* for 30–40 min at room temperature, followed by triplicate washes. Bone marrow cells were collected by flushing femurs with ice-cold PBS, and single-cell suspensions were prepared by passage through a 26-gauge needle. For baboons, peripheral blood was obtained from the femoral vein of baboons anaesthetized with an intramuscular injection of 10 mg kg^{-1} ketamine hydrochloride (Bionichepharma). Blood was collected into 10-ml sterile EDTA vacutainers (Becton Dickinson) and transported on ice to IUSM for analysis. Complete blood counts with differentials were performed on a Hemavet 950FS. Peripheral blood was then diluted 1:3 with PBS and mononuclear cells were isolated using Ficoll-Paque Plus (Amersham Biosciences), per manufacturer's protocol.

Colony assays. Bone marrow cells or PBMCs were resuspended in McCoy's 5A modified media supplemented with 100 U ml^{-1} penicillin, 100 µg ml^{-1} streptomycin, 0.6× modified essential medium (MEM) vitamin solution, 1 mM sodium pyruvate, 0.8× MEM essential amino acids, 0.6× MEM non-essential amino acids, 0.05% sodium bicarbonate (all from Gibco), serine, asparagine, glutamine mixture and 15% HI-FBS (Hyclone Sterile Systems) as described[30,31]. Cells were mixed with 0.3% agar (Difco Laboratories) in McCoy's 5A medium with 10 ng ml^{-1} rhGM-CSF and 50 ng ml^{-1} rmSCF (R&D Systems). PBMCs were cultured at 2×10^5 cells per ml and bone marrow cells at 5×10^4 cells per millilitre. All cultures were established in triplicate from individual animals, incubated at 37 °C, 5% CO_2, 5% O_2 in air for seven days and colonies were quantified by microscopy. In some experiments, total CFC including CFU-GM, BFU-E and CFU-GEMM were enumerated in 1% methylcellulose/IMDM media containing 30% FBS, 1 U ml^{-1} recombinant human erythropoietin (EPO), 10 ng ml^{-1} rhGM-CSF or rmGM-CSF and 50 ng ml^{-1} rhSCF or rmSCF as described[32,33]. In some experiments, phenotypically defined common myeloid progenitor (CMP) and granulocyte–macrophage progenitor (GMP) were plated at 500 cells per plate and colony growth determined in agar CFC assays with rmGM-CSF plus rmSCF or rmM-CSF. For analysis of CFC in baboons, similar assays were performed using recombinant human growth factors.

Flow cytometry. All antibodies were purchased from BD Biosciences unless otherwise noted. For detection of SKL cells, we used streptavidin conjugated with phycoerythrin (PE)-Cy7 (to stain for biotinylated MACS lineage antibodies (Miltenyi)), c-kit-allophycocyanin (APC), Sca-1-PE or APC-Cy7, CD45.1-PE or CD45.2-FITC. For SLAM SKL, we used Sca-1-PE-Cy7, c-kit-FITC, CD150-APC (eBiosciences), CD48-biotin (eBiosciences) and streptavidin-PE. CXCR4 expression was analysed using biotinylated lineage antibodies, streptavidin-PE-Cy7, c-kit-APC, Sca-1-APC-Cy7 and CXCR4-PE. For baboon CD34 analysis, CD34-PE (clone 563) was used. For macrophages, antibodies against CD115 (clone AFS98), Gr-1 (clone RB6-8C5) and F4/80 (clone CI:A3-1) were used. Osteolineage populations were identified and sorted as previously described[19]. For enumeration of bone marrow endothelial cells, femurs and tibias were crushed in a sterile mortar, and digested in collagenase (0.3%) at 37 °C for 1 h. Recovered cells were co-stained with fluorochrome-conjugated antibodies against CD45, Ter119, Sca-1, VEGFR3 and CD31, and the total number of sinusoidal endothelial cells (SECs; CD45$^-$ Ter119$^-$ Sca-1$^-$ VEGFR3$^+$ CD31$^+$) per femur was enumerated by flow cytometry analysis. To examine endothelial cell apoptosis, gated CD45$^-$ Ter119$^-$ Sca-1$^-$ VEGFR3$^+$ CD31$^+$ cells were stained with annexin V (BD Biosciences) and LIVE/DEAD staining dye (Invitrogen). For enumeration of myeloid progenitors (CMP, GMP and megakaryocyte–erythroid progenitors (MEP)), femurs and tibias were flushed with 5 ml IMDM containing 2% FBS. Lineage-positive cells were depleted using the lineage-cell depletion kit (Miltenyi Biotec), and lineage-negative cells were stained with fluorochrome-conjugated antibodies against Sca-1, c-Kit, IL-7Rα, CD34 and FCRγll/lll and analysed by flow cytometry. The Lin$^-$ IL-7Rα$^-$ Sca-1$^-$ c-Kit$^+$ fraction was subdivided into three subpopulations, CMP (FCRγll/lll^{low}CD34$^+$), MEP (FCRϒll/lll^{low} CD34$^-$), and GMP (FCRϒll/lll^{hi}CD34$^-$), and collected by sorting. All flow cytometry analyses were performed on an LSRII flow cytometer (BD). Cell sorting was performed on a BD Aria or Reflection II or Reflection III sorters.

Peripheral blood mobilization. Several different mobilization strategies were used, with specific details of dosing and schematics of dosing regimens shown on the data figures or included in the figure legends. In general, mice were given subcutaneous treatments of vehicle, NSAIDs (at varying doses), G-CSF (50 µg kg^{-1}, twice a day for four days), or G-CSF plus NSAIDs. For studies exploring mobilizing agents other than G-CSF, mice were treated with AMD3100 (5 mg kg^{-1} at day five; single injection), and peripheral blood was collected 1 h after AMD3100 treatment. For comparisons of several different NSAIDs, all NSAIDs were dosed by oral gavage using an enhanced oral gavage technique[34]. Each gavage treatment was given in a 0.2-ml bolus (10 ml kg^{-1}) of 0.5% methyl cellulose (Sigma-Aldrich) with an NSAID suspended in solution. For E-prostanoid receptor analysis, mice were mobilized with G-CSF in combination with meloxicam, AH6809 (EP1–3 antagonist, 10 µg per mouse, intraperitoneally, four days), AH23848 (EP4 antagonist, 10 µg per mouse, intraperitoneally, four days), L-161,982 (EP4 antagonist, 10 µg per mouse, intraperitoneally, four days) or G-CSF plus meloxicam and an EP2, EP1/3 or EP4 agonist (10 µg per mouse, intraperitoneally, four days) or dmPGE$_2$ (10 µg per mouse, intraperitoneally, four days). For baboon studies, a baseline bleed was performed for CBC, CD34 and CFC analysis. Two days later, two baboons were treated with 10 µg kg^{-1} G-CSF, and two baboons were treated subcutaneously with 10 µg kg^{-1} G-CSF and 0.2 mg kg^{-1} meloxicam on day 1, followed by 0.1 mg kg^{-1} meloxicam for subsequent days, for a total of five days. Blood was collected after the treatment regimen for CBC, CD34 and CFC analysis. After a two-week resting period, the above procedure was repeated, switching treatment groups for individual baboons. Furthermore, after another two-week resting period, blood was collected before and after a five-day treatment regimen with meloxicam, and CBC, CD34 and CFC were analysed. For healthy volunteer studies, subjects naive to any medications within 30-days received a baseline bleed, followed by a second bleed after a five-day regimen of 15 mg meloxicam per day, orally. CD34 cells were assessed by the International Society of Hematotherapy and Graft Engineering (ISHAGE) procedure[35] performed by the Stem Cell Laboratory of the IUSM Bone Marrow Transplant Program. CFC were assessed as described above.

Limiting dilution competitive transplantation. CD45.1 mice were mobilized with a standard four-day regimen of G-CSF, or G-CSF plus a four-day regimen of meloxicam (6 mg kg^{-1}). In some studies designed to evaluate timing and duration of NSAID dosing in combination with G-CSF, initiation of the NSAID regimen preceded G-CSF treatement and was staggered such that NSAID administration ended simultaneous with the G-CSF regimen (no stagger), one day before G-CSF (1-day stagger) or two days before G-CSF (2-day stagger) (regimens as depicted in the corresponding data figure). On day 5, PBMCs were acquired and transplanted at 1:1, 2:1, 3:1 or 4:1 ratios with 5×10^5 C57Bl/6J WBM competitors into lethally irradiated C57Bl/6J recipient mice. Peripheral blood chimaerism was monitored monthly, and CRU and LT-HSC frequency calculated. Transplants to evaluate LT-HSC mobilized in *Opn*$^{-/-}$ mice or with EP4 antagonist were performed competitively at a 4:1 ratio; 800,000 PBMCs from CD45.2 mice versus 200,000 WBM from CD45.1 mice and peripheral blood chimaerism and multilineage reconstitution were assessed 16 weeks after transplantation.

Recovery assay. Mice were mobilized with G-CSF or G-CSF plus meloxicam with staggered dosing as described above, and 2×10^6 mobilized PBMCs were transplanted non-competitively into cohorts of ten lethally irradiated recipients per group. A cohort of non-irradiated mice was bled on the same schedule as the experimental-treated groups of mice. Every other day, five mice from each group were bled (~50 µl from a tail snip), and neutrophils and platelets in blood were enumerated using a Hemavet 950FS. Alternative groups of five mice were bled on each successive bleeding time point so that mice were only bled once every four days. Recovery of neutrophils and platelets to 50% and 100% were determined by comparison to the average neutrophil and platelet counts in the control group throughout the experimental period. After 90 days, mice were euthanized, bone marrow was collected and transplanted at a 2.5:1 ratio with 2×10^5 congenic competitors into lethally irradiated recipients to determine long-term repopulating ability of the primary mobilized graft.

EP4 chimaera generation and mobilization assay. Chimeras were generated using *EP4*$^{Cre;flox/flox}$ mice and age- and sex-matched *EP4*$^{flox/flox}$ littermate controls. *EP4*$^{flox/flox}$ mice were lethally irradiated and transplanted with 2×10^6 WBM cells from either

EP4$^{flox/flox}$ mice, allowing for generation of a wild-type:wild-type chimaera, or from *EP4*$^{Cre;flox/flox}$ mice, allowing for generation of a knockout:wild-type chimaera. Similarly, *EP4*$^{Cre;flox/flox}$ mice were lethally irradiated and transplanted with 2×10^6 WBM cells from *EP4*$^{flox/flox}$ mice, allowing for generation of a wild-type:knockout chimaera. At 8 weeks after transplantation, all mice were treated with 2 mg tamoxifen for three consecutive days, rested for three days and injected for three more days. Mice were then treated with G-CSF or G-CSF plus meloxicam starting ten days after the last treatment, and peripheral blood CFC and SLAM SKL were assessed as described. *EP4* gene deletion was confirmed by qRT–PCR.

qRT–PCR. For E-prostanoid receptor expression on sorted osteolineage cells, total RNA was extracted with the purelink RNA micro kit (Invitrogen). On-column DNase treatment was performed according to the manufacturer's instructions to eliminate contaminating genomic DNA. Conventional reverse transcription was followed with SuperScript III first-strand synthesis system (Invitrogen). qRT–PCR was performed using the SYBR advantage qPCR Premix kit (Clontech) on MxPro-3000 (Agilent). Primers were synthesized at IDT (Supplementary Table 1). A primer concentration of 250 nM was found to be optimal in all cases. The PCR protocol consisted of one cycle at 95 °C (5 min) followed by 45 cycles of 95 °C (15 s), 55 °C (30 s) and 72 °C (30 s). The dissociation curves were determined on each analysis to confirm that only one product was obtained. Expression of glyceraldehyde-3-phosphate dehydrogenase (*GAPDH*) and hypoxanthine guanine phosphoribosyl transferase (*HPRT*) were used as reference genes. The average threshold cycle number (C_t) for each tested mRNA was used to quantify the relative expression of each gene. For analysis of haematopoietic supportive molecules on sorted osteolineage cells from vehicle-treated or NSAID-treated mice, qRT–PCR was performed with the TaqMan gene expression assay kit (Life Technologies) (Supplementary Table 2), with complementary DNA generated from the high capacity cDNA reverse transcription kit (Life Technologies). Microfluidic qRT–PCR was performed on BioMark Dynamic Arrays according to manufacturer's instructions (Fluidigm Corporation).

Micro-computed tomography. Formalin-fixed tibiae and femora were imaged with micro-computed tomography using a microCT-viva 40 (Scanco Medical AG) with a voxel size of 10.5 μm in all dimensions ($n = 5$). The bones were mounted in a cylindrical specimen holder to be captured in a single scan. Bones were secured in the specimen holder with gauze and were completely submerged in 70% ethanol. The region of interest comprised 100 transverse computed tomography slices. Scans with an isotropic resolution of 10.5 μm were made using a 55-kV peak voltage X-ray beam. The fractional trabecular bone volume (BV/TV) and architectural properties of trabecular reconstructions, apparent trabecular thickness (Tb.Th.), trabecular number (Tb.N.), trabecular spacing (Tb.Sp.), and connectivity density (Conn.D.) were calculated.

Dynamic and static bone histomorphometry. Dynamic bone formation assays were performed using staggered calcein double labelling, as described previously[36]. Bone histomorphometry was performed on 7-μm thick sections of undecalcified femurs embedded in methylmethacrylate using standard procedures. The mineral apposition rate (mm per day), mineralizing surface and bone formation rate (mm^3 mm^{-2} per day) were measured on femora. Modified Goldner's trichrome staining procedure was performed on 7-μm thick sections of undecalcified femurs embedded in methylmethacrylate. The osteoid surfaces as well as quiescent surfaces were measured on the tissue sections. Bone marrow sinusoids were visualized with anti-VEFGFR3 on 3.5-μm section. Vessels were identified by the positive staining around the vessel walls, and vessel areas were measured using the automated measuring system and expressed as a percentage or tissue volume. Vessel surface was traced with the same automated system. Vessel wall that showed an intact epithelial surface was expressed as endothelial surface over total vessel surface. For Col2.3-GFP analysis, 3.5-μm thick sections were obtained from treated Col2.3-GFP mice. Sections were visualized with a fluorescent microscope (Leica D100) using a FITC filter. Images were captured at ×400 magnification at four different areas in the mid-shaft of the femur. GFP$^+$ osteoblasts were counted on endocortical bone surfaces, and data were expressed as the number of osteoblasts per endocortical bone surface. Osteoblast surface was measured and expressed as the endocortical bone surface covered by osteoblasts. All histomorphometry experiments were done on images captured using a Leica microscope outfitted with Q-imaging camera (W. Nuhsbaum), and the histomorphometry analysis was done using Bioquant Osteo software automated measuring system (Bioquant Imaging Corporation). All histomorphometry values were expressed according to the standard nomenclature[37,38].

Immunohistochemistry. Immunohistochemical analysis was performed on decalcified paraffin-embedded tissue sections. Rabbit polyclonal antibodies against N-cadherin and SDF1 N-terminal were from Abcam. Secondary anti-rabbit antibodies were from Vector Laboratories. Anti-mouse OPN was from R&D Systems. Secondary biotinylated anti-goat horseradish peroxidase (HRP) conjugate, HRP-DAB system and DAV chromogen were from R&D Systems. HRP–rat IgG2 isotype was used as a primary antibody negative control for SDF-1, OPN and N-cadherin, at 1:50. Isotype staining control was performed under the same conditions as the antibody staining.

COX metabolite and activity analysis. Mice were subcutaneously treated with vehicle control or meloxicam, twice daily. One hour after the last treatment, femurs were pulled and flushed with 1 ml of ice-cold PBS, quickly brought to single-cell suspension and then flash frozen. COX-1- and COX-2-derived metabolites were assessed by gas chromatography–mass spectrometry as we have previously described[39,40]. The second femur was processed in an identical way, and COX-1 and COX-2 activity were determined using a fluorescent COX activity assay following the manufacturer's instructions (Cayman Chemicals).

27. Mignone, J. L., Kukekov, V., Chiang, A. S., Steindler, D. & Enikolopov, G. Neural stem and progenitor cells in nestin-GFP transgenic mice. *J. Comp. Neurol.* **469,** 311–324 (2004).
28. Kalajzic, Z. *et al.* Directing the expression of a green fluorescent protein transgene in differentiated osteoblasts: comparison between rat type I collagen and rat osteocalcin promoters. *Bone* **31,** 654–660 (2002).
29. Chen, X. S., Sheller, J. R., Johnson, E. N. & Funk, C. D. Role of leukotrienes revealed by targeted disruption of the 5-lipoxygenase gene. *Nature* **372,** 179–182 (1994).
30. King, A. G. *et al.* Rapid mobilization of murine hematopoietic stem cells with enhanced engraftment properties and evaluation of hematopoietic progenitor cell mobilization in rhesus monkeys by a single injection of SB-251353, a specific truncated form of the human CXC chemokine GROβ. *Blood* **97,** 1534–1542 (2001).
31. Pelus, L. M., Broxmeyer, H. E., Kurland, J. I. & Moore, M. A. Regulation of macrophage and granulocyte proliferation. Specificities of prostaglandin E and lactoferrin. *J. Exp. Med.* **150,** 277–292 (1979).
32. Broxmeyer, H. E. *et al.* SDF-1/CXCL12 enhances in vitro replating capacity of murine and human multipotential and macrophage progenitor cells. *Stem Cells Dev.* **16,** 589–596 (2007).
33. Fukuda, S., Bian, H., King, A. G. & Pelus, L. M. The chemokine GROβ mobilizes early hematopoietic stem cells characterized by enhanced homing and engraftment. *Blood* **110,** 860–869 (2007).
34. Hoggatt, A. F., Hoggatt, J., Honerlaw, M. & Pelus, L. M. A spoonful of sugar helps the medicine go down: a novel technique to improve oral gavage in mice. *J. Am. Assoc. Lab. Anim. Sci.* **49,** 329–334 (2010).
35. Sutherland, D. R., Anderson, L., Keeney, M., Nayar, R. & Chin-Yee, I. The ISHAGE guidelines for CD34$^+$ cell determination by flow cytometry. *J. Hematother.* **5,** 213–226 (1996).
36. Mohammad, K. S. *et al.* Pharmacologic inhibition of the TGF-β type I receptor kinase has anabolic and anti-catabolic effects on bone. *PLoS ONE* **4,** e5275 (2009).
37. Rowe, P. S. *et al.* Correction of the mineralization defect in hyp mice treated with protease inhibitors CA074 and pepstatin. *Bone* **39,** 773–786 (2006).
38. Parfitt, A. M. *et al.* Bone histomorphometry: standardization of nomenclature, symbols, and units. Report of the ASBMR Histomorphometry Nomenclature Committee. *J. Bone Miner. Res.* **2,** 595–610 (1987).
39. Murali, G. *et al.* Fish oil and indomethacin in combination potently reduce dyslipidemia and hepatic steatosis in *LDLR*$^{-/-}$ mice. *J. Lipid Res.* **53,** 2186–2197 (2012).
40. Liu, T. *et al.* Prostaglandin E_2 deficiency uncovers a dominant role for thromboxane A_2 in house dust mite-induced allergic pulmonary inflammation. *Proc. Natl Acad. Sci. USA* **109,** 12692–12697 (2012).